Imaging with multiples using linearized full-wave inversion

Mandy Wong, Biondo Biondi, and Shuki Ronen

ABSTRACT

We presents a technique for imaging both primaries and multiples using linearized inversion. When used with a suitable migration velocity model, linearized full-wave inversion (LFWI) makes use of the multiple energy as signal while removing the crosstalk in the image. By using the two-way propagator in both modeling and migration, we can image a class of multiply scattered events. Such events can scatter off sharp-interfaces in the migration velocity many times but only interact with the (reflectivity) model once. We demonstrate the concept and methodology in 2D with a synthetic Sigsbee2B model.

INTRODUCTION

Traditionally, seismic imaging techniques only account for the primary reflections. In the presence of strong reflectors (e.g.. air-water interface, hard water bottom or salt bodies), multiples can significantly degrade the interpretation of images. Therefore, much effort has been devoted to developing multiple suppression techniques in the past few decades.

The well-known multiple-removal tools such as deconvolution (in time, frequency, and slant-stack domains), Radon-transform demultiple and frequency-wavenumber (f-k) demultiple are limited unless the geology of the subsurface is simple. In the presence of complex geology, multiples are not totally separable from primaries by criteria such as periodicity, moveout velocity, and spectra. In model-based technique, which predict multiples with wavefield extrapolation (Morley, 1982; Berryhill and Kim, 1986; Wiggins, 1988; Lu et al., 1999), the accuracy of the predicted multiples strongly depends on the model used. Surface-related multiple elimination (SRME), a convolution-based technique (Riley and Claerbout, 1976; Tsai, 1985; Verschuur et al., 1992), is more generally applicable. But this method requires an overlap of source and receiver locations and cannot suppress internal multiples. Despite substantial progress in multiple elimination, complete removal of surface-related and internal multiples without distorting the primary signals remains a challenge.

One motivation to make use of multiples is that they can provide subsurface information not found in primaries. For a given pair of source and receiver, the sub-surface reflection point of a multiple is located differently than that of a primary. For a multi-shot seismic survey, migrating the multiples translates to higher fold for regions well

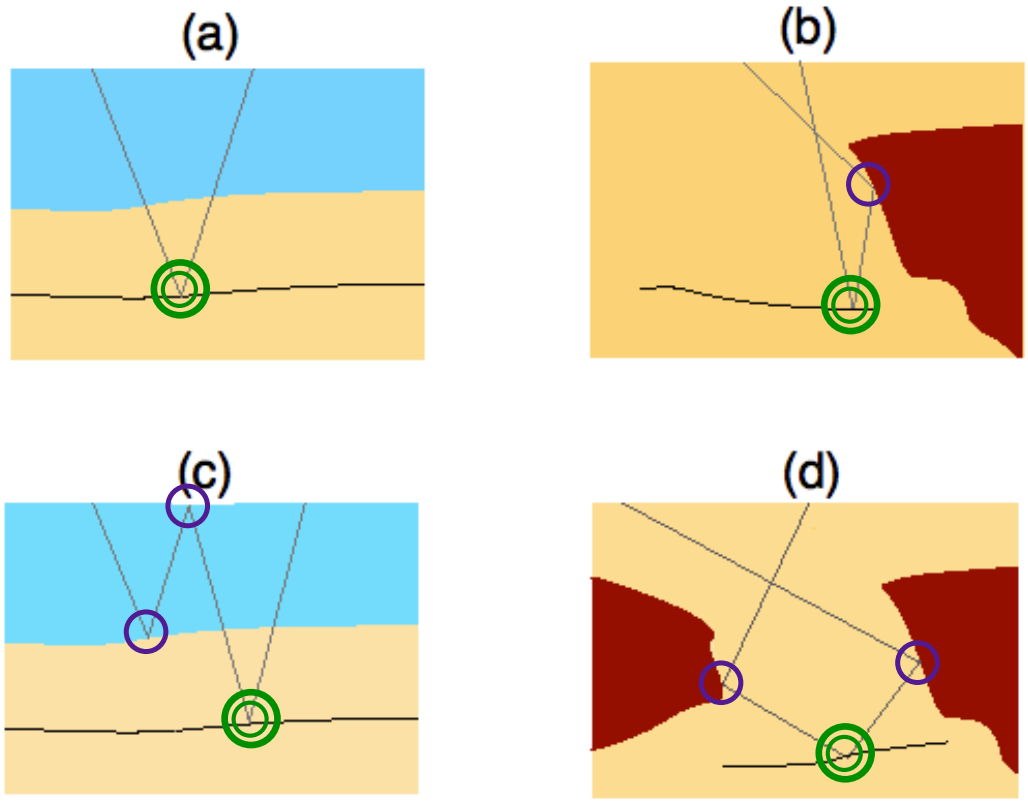

Figure 1: The ray-path for a (a) singly scattered event, (b) a doubly scattered event and (c,d) triply scattered events. Single circles (in purple) indicate scattering off the migration velocity while double circle (in green) indicate scattering off the model $m(\mathbf{x})$. [**NR**]

imaged by the primaries and more subsurface illumination for regions not covered by the primaries. In addition, despite the advance of multiple suppression techniques, complete removal of all multiples from the primaries still remains a challenge. Migrating such signals would result in *crosstalk* artifacts. Finally, multiples are even more sensitive to velocity information than the primaries, because they travel a longer path in the subsurface. Multiple signals can potentially be used as part of an iterative velocity building tool. Reiter et al. (1991) made an early attempt to capitalize on the potential of multiples by formulating a prestack Kirchhoff time-migration method that includes the first-order water-layer reverberation in the migration operator. Because ocean bottom cable data could not be decomposed into up- and down-going components at the time, such work was limited to deep water datasets.

When surface-related multiples have been explicitly separated from the primary reflections (e.g., using SRME), they can be imaged independently from the primary reflections by using shot-profile (Guitton, 2002) or source-receiver (Shan, 2003) depth migration. Muijs et al. (2007) image primary and free-surface multiples for OBS data by decomposing data into up-going and down-going constituents, followed by

downward extrapolation and a 2D deconvolution-based imaging condition. All these techniques image the surface-related multiples by transforming the primary signal into a pseudo-source for migration with the multiple signals using the one-way wave equation. Recently, Liu et al. (2011) extend the technique to the two-way wave equation. While these techniques are computationally efficient, their images contain crosstalk artifacts caused by the interference of wavefields not associated with the same subsurface reflector. A robust technique is needed to get the benefit of multiple imaging without compromising image quality. We propose using linearized full-wave inversion (LFWI) to use multiple energy as signal while removing the crosstalk in the image.

In the next section, we discuss how to image with multiples with LFWI for the streamer geometry and the OBN geometry. We then show the results of our inversion scheme from a layered model and a 2D Sigsbee2B model for the OBN geometry.

THEORY

LFWI poses the imaging problem as an inversion problem by linearizing the wave-equation with respect to our model ($m(\mathbf{x})$). We define our model to be a weighted difference between the migration slowness ($s_o(\mathbf{x})$) and the true slowness ($s(\mathbf{x})$):

$$m(\mathbf{x}) = (s(\mathbf{x}) - s_o(\mathbf{x}))s_o(\mathbf{x}) \tag{1}$$

Assuming that the earth behaves as a constant-density acoustic isotropic medium, we linearize the wave equation and apply the first-order Born approximation to get the following forward modeling equation:

$$d^{mod}(\mathbf{x}_r, \mathbf{x}_s, \omega) = \sum_{\mathbf{x}} \omega^2 f_s(\omega) G(\mathbf{x}_s, \mathbf{x}, \omega) m(\mathbf{x}) G(\mathbf{x}, \mathbf{x}_r) \tag{2}$$

where d^{mod} represents the forward modeled data, ω is the temporal frequency, $m(\mathbf{x})$ is a function of the image point $\mathbf{x}$, $f_s(\omega)$ is the source waveform, and $G(\mathbf{x}_s, \mathbf{x})$ is the Green's function of the two-way acoustic constant-density wave equation over the migration slowness. Note that G is actually ω-dependent and is a function of $s_o(\mathbf{x})$ only. It is important to point out that the adjoint of the forward-modeling operator is the migration operator:

$$\mathbf{m}_{mig}(\mathbf{x}) = \sum_{\mathbf{x}_r, \mathbf{x}_s, \omega} \omega^2 f_s^*(\omega) G^*(\mathbf{x}_s, \mathbf{x}, \omega) G^*(\mathbf{x}, \mathbf{x}_r) d(\mathbf{x}_r, \mathbf{x}_s, \omega) \tag{3}$$

The inversion problem is defined as minimizing the least-squares difference between the synthetic and the recorded data:

$$S(\mathbf{m}) = \|\mathbf{L}\mathbf{m} - \mathbf{d}\|^2 = \|\mathbf{d}^{mod} - \mathbf{d}\|^2 \tag{4}$$

where $\mathbf{L}$ is the forward-modeling operator that corresponds to equation 2.

At first glance, equation 2 seems to only generate singly scattered events (e.g. Figure 1 a). To clarify, the term scattering includes both diffraction and reflection. However, if we construct our propagator ($G(\mathbf{x}, \mathbf{y})$) using the two-way wave equation, equation 2 can actually generate multiply scattered events. In figure 1 b, the ray path reflects off a salt flank and then the horizontal reflector. If the sharp salt-flank boundary already exists in the migration velocity, then the scattering off the salt flank is automatically generated by the propagator (Green's function). Figure 1 (c) and (d) shows two triply scattered events. Single circles (in purple) show scattering off the migration velocity, while double circles (in green) show scattering off the model $m(\mathbf{x})$.

Multiple imaging with towed streamer

For a towed-streamer geometry, one only needs to introduce (i) the free-surface and (ii) sharp boundaries into the migration velocity $s_o(\mathbf{x})$ to begin modeling both primaries and multiples. If the sea-bottom has a sharp interface in $s_o(\mathbf{x})$, then equation 2 can model all surface-related multiples as shown in Figure 2 (a). The same is true for ocean-bottom data, which we will discuss next.

Multiple imaging with ocean-bottom node

In an ocean-bottom survey, the signal (Figure 3) can be classified into up-going (in red) and down-going signal (in grey) with respect to the receivers. The lowest order of the up-going signal is the primary reflection. The lowest order of the down-going signal is the direct-arrival. Since the direct-arrival does not carry any information about the subsurface, the next order of down-going event, the mirror signal, is used for conventional migration of down-going OBN data.

We will referred the mirror signal as the down-going primary from now on. This is not to be confused with the up-going primary. One can apply LFWI on the ocean-bottom hydrophone recording without decomposing the up- and down-going signal. However, using only the hydrophone without up-down decomposition for imaging is less favorable due to the following reasons:

1. The migration image contains more crosstalk artifacts due to the migration of the up- and down-going modes. Although inversion can, in theory, push out the crosstalk artifacts, it requires more iterations.

2. The energy in the up-going primary is stronger than that in the down-going primary. If the up-down modes are not separated in the data space, it is difficult for the inversion to apply data weighting to balance the contribution from the two modes.

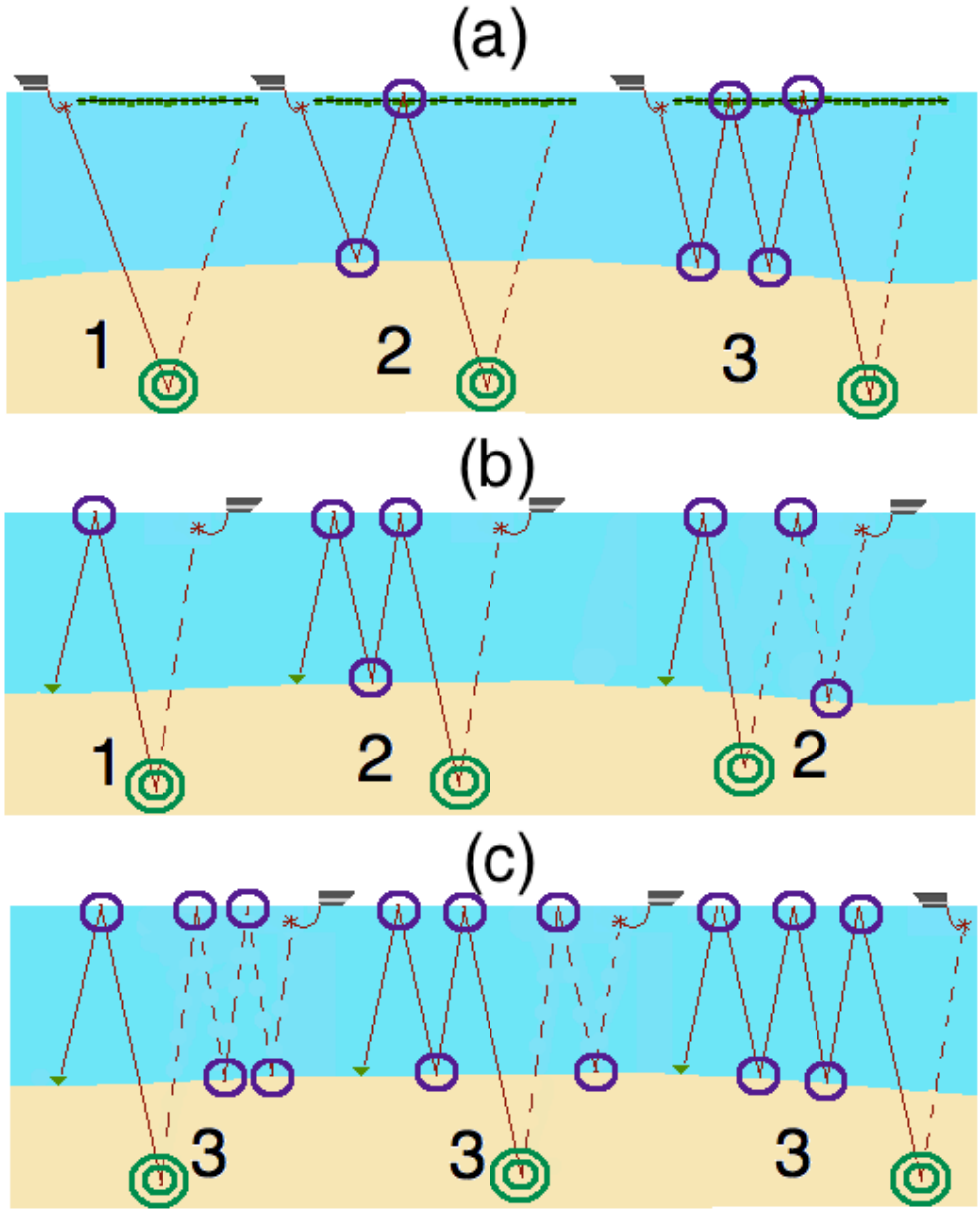

Figure 2: (a) Ray paths for the primary, the first-order, and the second-order multiples for the towed-streamer acquisition geometry. (b) Ray paths for the down-going mirror and the down-going first-order multiples for ocean-bottom-node acquisition. (c) Ray paths for the down-going second-order multiples for ocean-bottom-node acquisition. Purple-solid circles show scattering off either the free-surface or the background velocity model. Green-double circles show scattering off the reflectivity model. [**NR**]

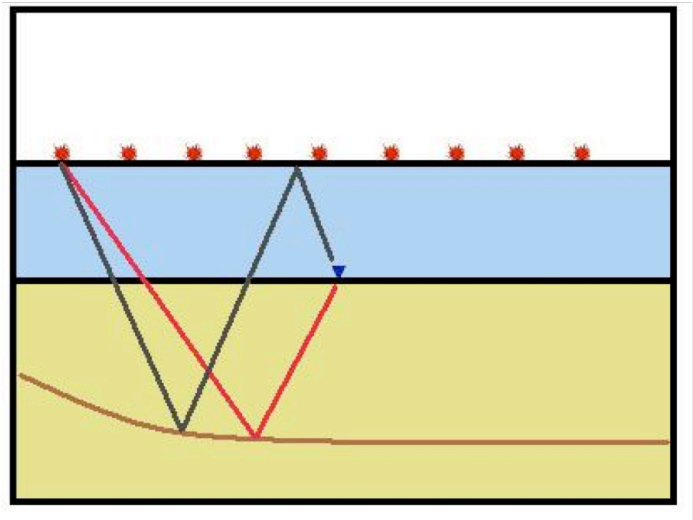

Figure 3: For a given pair of source and receiver, the sub-surface reflection point of a multiple event is different than that of a primary event. [**NR**]

3. Up-down decomposition by PZ summation can alleviate loss signal at the notch frequencies. A benefit that is loss if imaging only with the hydrophone.

In this study, we focus on imaging different orders of down-going signals as shown in Figure 2 b and c. To simulate the final down-going leg of the wave path, an areal shot is pre-calculated by first injecting the source wavelet at the receiver location, letting the wavefield propagate, and then capturing the signal at the sea surface (Figure 4). To generate the incident wavefield, the saved areal shot is re-injected at the sea-surface with a -1 factor. The re-injected signal is then allowed to travel back and forth in the water column using a reflecting top boundary and a well-defined velocity contrast at the sea-bottom. This algorithm can correctly simulate the ray path traversed by the down-going primary and higher-order multiples.

The focus of this report is on imaging the higher-order multiples for OBN data with the method illustrated in Figure 4. In particular, we compare the image output between migration with the down-going primary and LFWI with both the down-going primary and the down-going multiples.

SYNTHETIC EXAMPLE

We apply LFWI on two models. The first one is a simple one-layered model that allows us to keep track of different kinds of migration artifacts. The second model is the more complicated Sigsbee2B model.

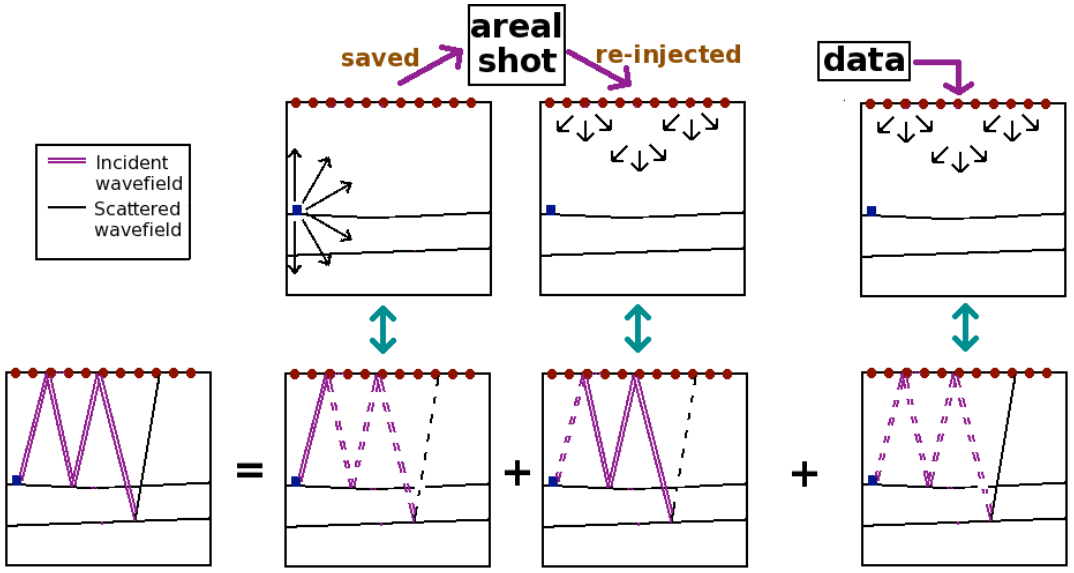

Figure 4: Illustration on the migration of the second-order signal. For the incident wavefield, an areal shot is pre-calculated to simulate the final down-going leg of the wave path. To generate the incident wavefield, the saved areal shot is re-injected at the sea-surface with a -1 factor. The re-injected signal is then allowed to travel back and forth in the water column using a reflecting top boundary and a well-defined velocity contrast at the sea-bottom. [**NR**]

One-layered model

We construct a one-layered model (Figure 5 a) with ocean-bottom geometry. The only sharp interface in the migration velocity is the seabed. Figure 5 b shows the synthetic data. The labels d_1, d_2 and d_3 correspond to the first, second, and third order events as shown in figure 2 b and c. Note that we used equation 2 to generate the synthetic data. Hence, internal multiples are absent. Figure 5 c shows the migration image m_{mig}. The migration image is made up of signal m_{sig} and crosstalk artifacts m_{xtalk}. In the figure, the label A indicates spurious reflectors generated by migrating the primary signal (d_1) as if it were a multiple. B is the correct reflector in the image. C is an artifact generated by migrating the multiple signal (d_2 or d_3) as if it were a primary reflection. In equation form, they are denoted as follows:

$$\begin{aligned} m_{mig} &= m_{signal} + [m_{xtalk}] = m_B + [m_A + m_C] \\ m_A &= \mathbf{L'}_2\mathbf{d}_1 + \mathbf{L'}_3\mathbf{d}_1 + \mathbf{L'}_4\mathbf{d}_1 + ... \\ m_B &= \mathbf{L'}_1\mathbf{d}_1 + \mathbf{L'}_2\mathbf{d}_2 + \mathbf{L'}_3\mathbf{d}_3 + ... \\ m_C &= \mathbf{L'}_1\mathbf{d}_2 + \mathbf{L'}_1\mathbf{d}_3 + \mathbf{L'}_2\mathbf{d}_3 + ... \end{aligned} \tag{5}$$

where m_A, m_B,and m_C correspond to the parts of the image labeled with A, B, and C in Figure 5 c. $\mathbf{L'}_1$, $\mathbf{L'}_2$, and $\mathbf{L'}_3$ are migration operators that correspond to

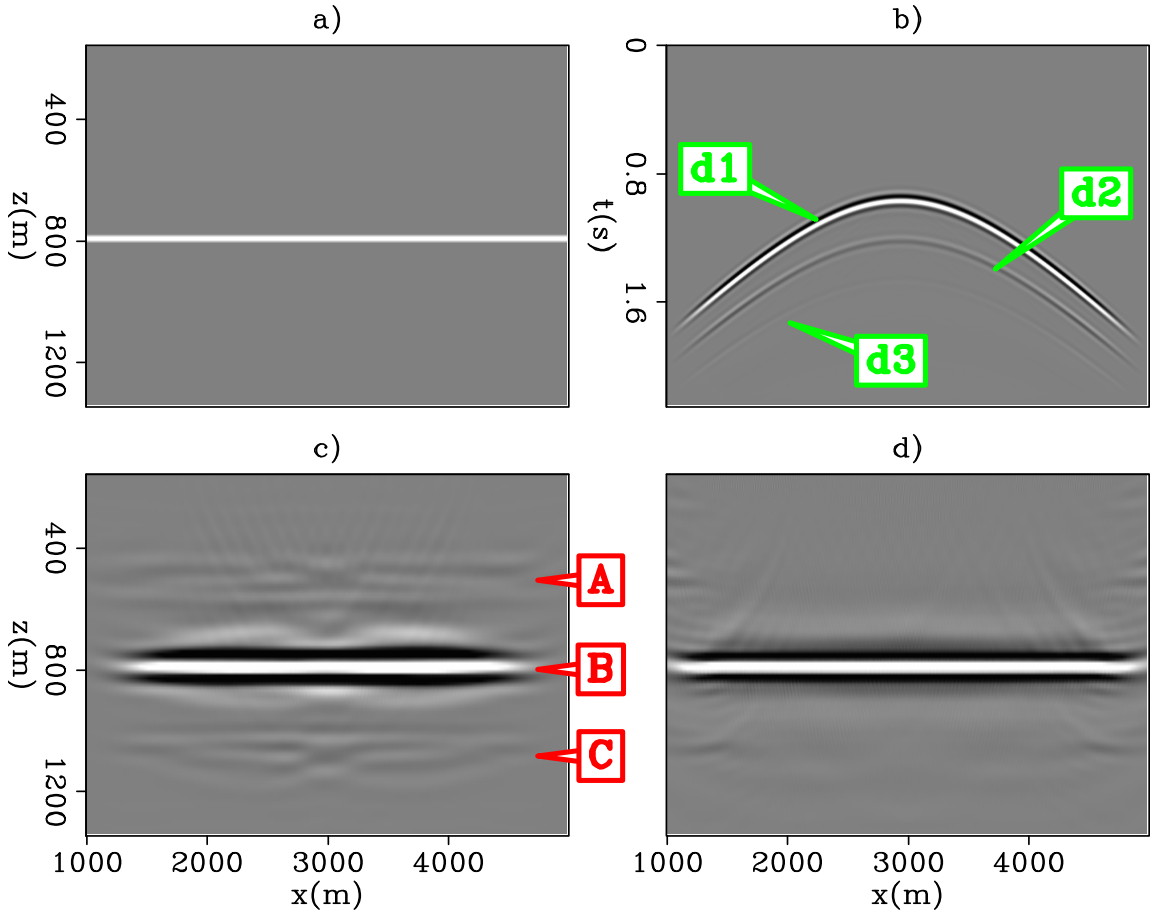

Figure 5: (a) Original one layered model, (b) synthetic data, (c) migration image and (d) inversion image. [**CR**]

different orders of reflection events. Figure 5 d shows the inversion result. Notice that the artifacts are removed from the image. In conventional imaging, if there were residual multiple energy in the data, then artifacts of type C would show up in the image. Treating those as real signal would negatively affect the interpretation of the sub-surface.

Sigsbee2B model

We apply LFWI to the Sigsbee2B model with the ocean-bottom geometry. Figure 7 shows the migration velocity and the reflectivity model used for this study. There are two interfaces in the migration velocity. One comes from the salt and the other comes from the basement reflector. These sharp interfaces along with the free surface boundary condition will generate the multiples. We first generate the down-going primary only data by applying the conventional mirror-imaging forward modeling operator. This is done by positioning the nodes at the mirror point across the sea-

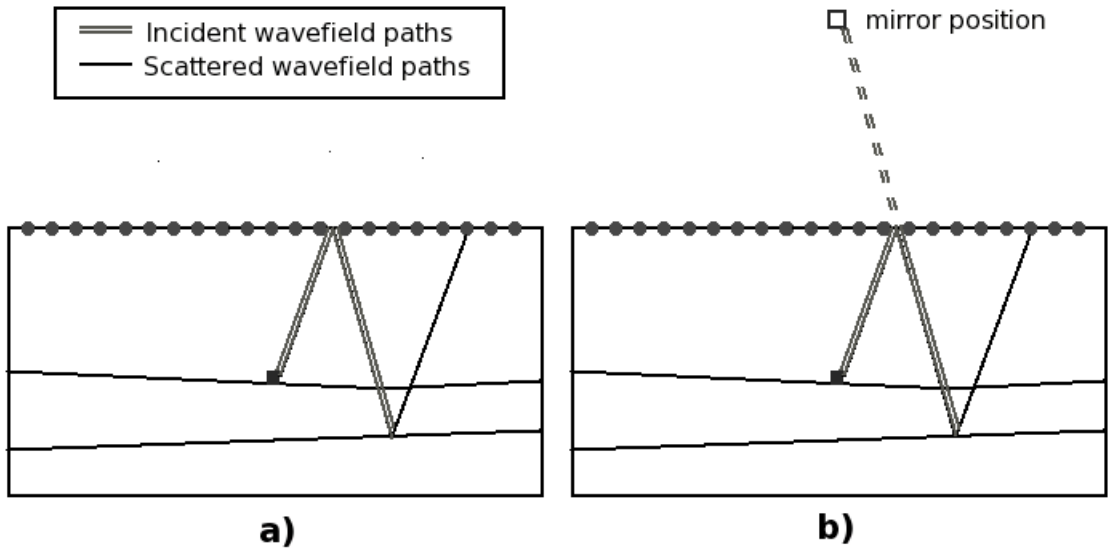

Figure 6: (a) The ray-path of a mirror signal. (b) The raypath of the same signal in mirror imaging. The apparent position of the receiver is not at twicce the ocean depth above the sea bed. This assumes the sea surface is a perfect reflector. Note that the top boundary is absorbing. [**NR**]

surface as shown in Figure 6. We then add 20 % of the down-going multiple energy to the down-going primary only data as shown in Figure 8. This is to simulate the case when multiple-elimination techniques cannot completely remove the multiples. We will refer to this synthetic simply as the *noisy primary* data. Figure 8 (b) shows the synthetic that contains first- and higher-order reflections. We will refer to this as the *primary-multiple* data.

Figure 9 shows the result of applying migration and linearized inversion to the data. Panel (a) is the conventional image in which we assume a primary-only migration operator on the primary data. The red arrow indicates the artifacts in the migration image that correspond to noise included with the primary. Panel (b) is the linearized inversion result with the primary-only operator. Note the substantial improvement between migration and inversion. It has been shown (Wong et al., 2011)that linearized inversion can enhance the resolution of the image, suppress the migration artifacts, and increase the relative amplitude of true reflectors. Next, panel (c) shows the migration result achieved by applying a primary-multiple migration operator to the primary-multiple data. There are many crosstalk artifacts in this image. Without addressing the crosstalk, it is difficult to argue that panel (c) is better than panel (a). Panel (d) is the linearized full-wave inversion (LFWI) result. The annotation indicates that LFWI can properly remove the crosstalk artifacts.

In terms of convergence, since this is a classical *inverse crime* study, our objective function decreases to two percent of its initial value after 40 iterations.

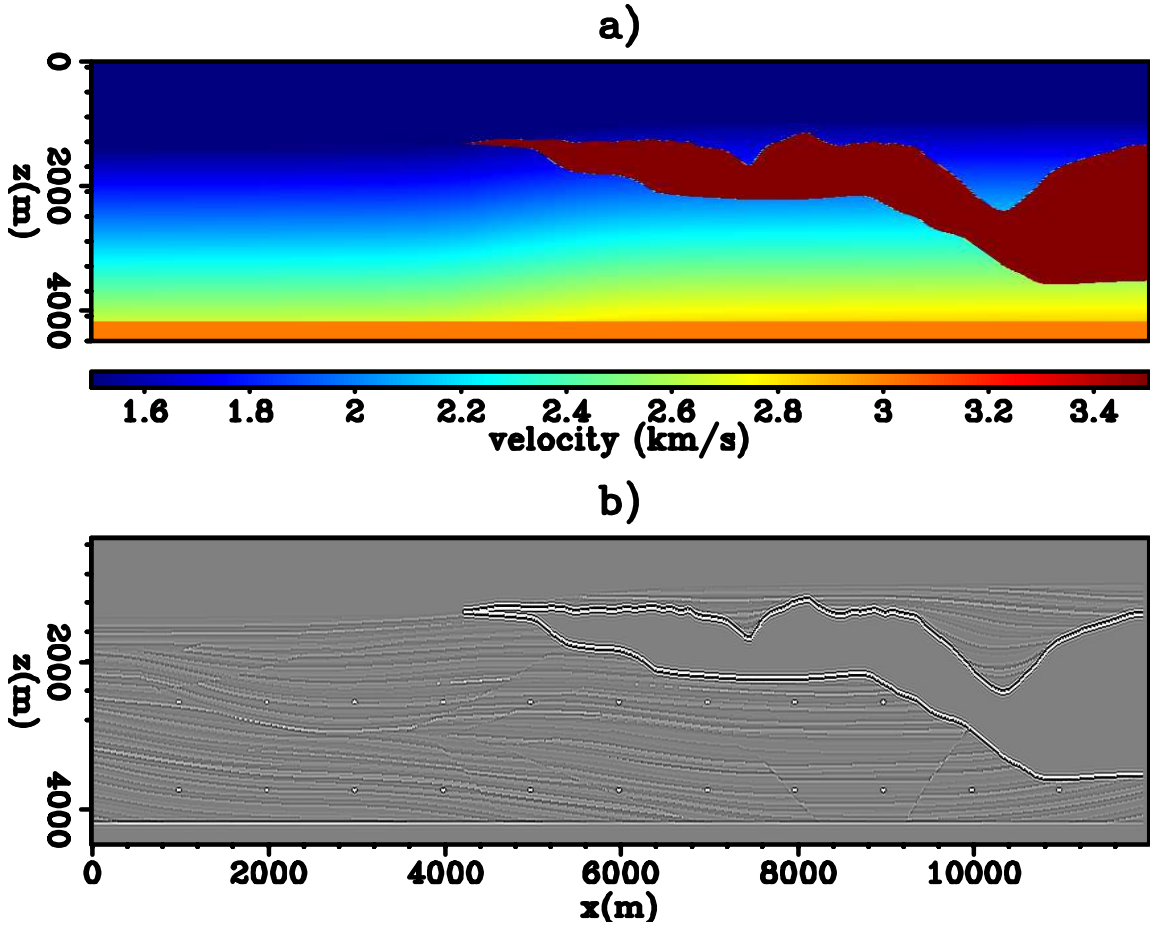

Figure 7: (a) Migration velocity model and (b) original reflectivity model. [**ER**]

DISCUSSION

Note that this technique does not migrate all orders of multiples. It only migrates multiples with a single scattering off the model $m(\mathbf{x})$ and other scattering off the sharp boundary in the migration velocity model. Considering that multiples with high amplitude in the data are often generated by sub-surface interfaces of high impedance contrast, this technique can account for most of the significant multiples in the data.

Our method is model-based. One obvious consideration is the accuracy of the migration velocity. A conservative way of applying LFWI would be to put in sharp interfaces that are easy to estimate (e.g. the free-surface, sea-bottom, and top-salt). However, what happens if there is a mis-positioned salt flank in the migration velocity? This may open an avenue for velocity estimation. As an imaging tool, LFWI works as well as other model-based multiple-prediction-subtraction methods.

We recommend applying LFWI for surveys where multiple removal is an issue. An appropriate field study for this method would be a shallow-water dataset with a deep

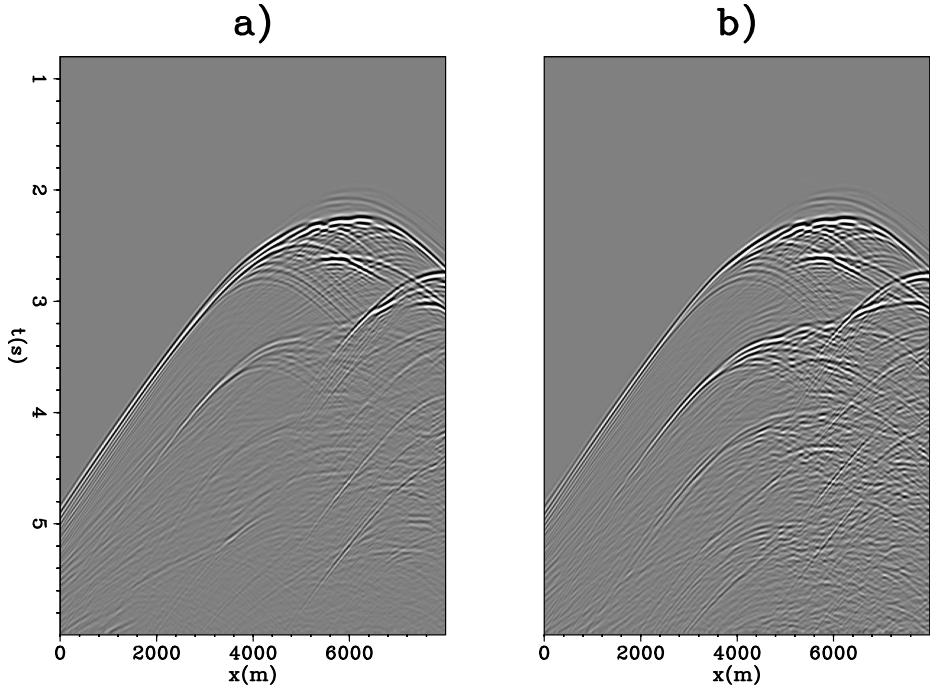

Figure 8: (a) The synthetic primary (lowest-order) data with 20 % multiple energy (*the noisy primary data*). (b) The primary and multiples synthetic data (*the primary-multiple data*). [**CR**]

target zone. In this case, each order of multiples overlaps with the previous order, and the conventional multiple-prediction-subtraction techniques might not deliver.

CONCLUSION

We demonstrated a method for imaging both primaries and multiples using linearized full-wave inversion (LFWI). LFWI not only increases the sub-surface illumination by using the multiple energy as signal, but also addresses the issue of crosstalk in the image. We demonstrate the concept and methodology with a 2D layered model and the Sigsbee2B model.

REFERENCES

Berryhill, J. L. and Y. C. Kim, 1986, Deep-water peglegs and multiples — emulation and suppression: Geophysics, **51**, 2177–2184.

Guitton, A., 2002, Shot-profile migration of multiple reflections: SEG Annual Meeting Expanded Abstracts, 1296–1299.

Liu, Y., X. Chang, D. Jin, R. He, H. Sun, and Y. Zheng, 2011, Reverse time migration of multiples: SEG Annual Meeting Expanded Abstracts, 3326–3330.

Lu, G., B. Ursin, and J. Lutro, 1999, Model-based removal of water-layer multiple reflections: Geophysics, **64**, 1816–1827.

Morley, L., 1982, Predictive multiple suppression: PhD thesis, Stanford University.

Muijs, R., J. Robertsson, and K. Holliger, 2007, Prestack depth migration of primary and surface-related multiple reflections: Part I - Imaging: Geophysics, **72**, S59–S69.

Reiter, E. C., M. N. Toksoz, T. H. Keho, and G. M. Purdy, 1991, Imaging with deep-water multiples: Geophysics, **56**, 1081–1086.

Riley, D. C. and J. F. Claerbout, 1976, 2D multiple reflections: Geophysics, **41**, 592–620.

Shan, G., 2003, Source-receiver migration of multiple reflections: SEG Annual Meeting Expanded Abstracts, 1008–1011.

Tsai, C. J., 1985, Use of autoconvolution to suppress first-order long period multiples: Geophysics, **50**, 1410–1425.

Verschuur, D. J., A. J. Berkhout, and C. P. A. Wapenaar, 1992, Adaptive surface-related multiple elimination: Geophysics, **57**, 1166–1177.

Wiggins, J. W., 1988, Attenuation of complex water-bottom multiples by wave equation-based prediction and subtraction: Geophysics, **53**, 1527–1539.

Wong, M., S. Ronen, and B. Biondi, 2011, Least-squares reverse time migration/inversion for ocean bottom data: A case study: SEG Expanded Abstracts, **30**, 2369–2373.

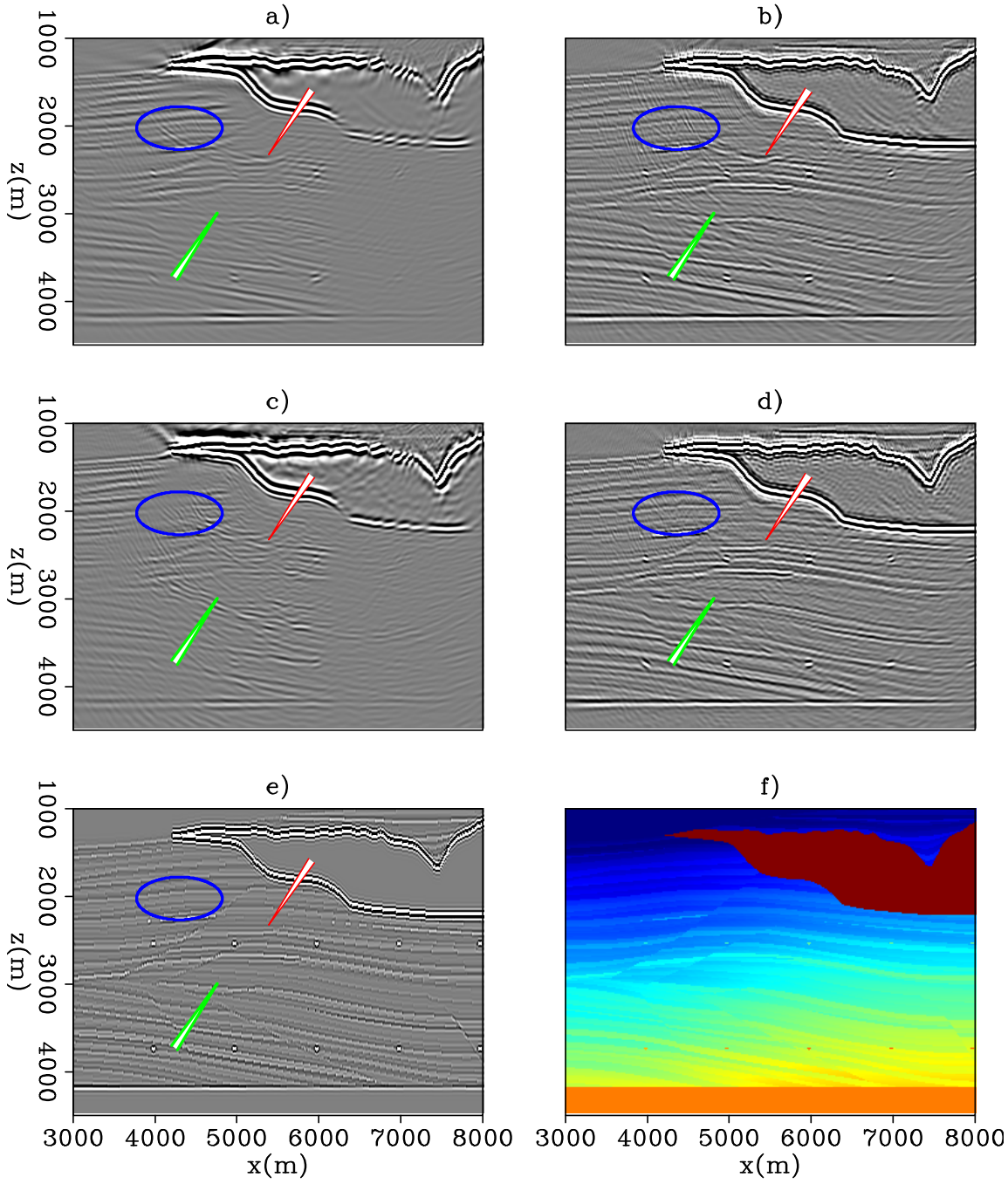

Figure 9: (a) Migration with the *noisy primary* data, (b) inversion with the *noisy primary* data, (c) migration with the *primary-multiple* data, (d) inversion with the *primary-multiple* data, (e) reflectivity model, and (f) velocity model. [**CR**]